Desalination and Water Treatment
www.deswater.com

doi: 10.5004/dwt.2019.24402

162 (2019) 364–375
September

Process optimization with Box–Behnken experimental design for photocatalytic degradation of thiamethoxam using perlite supported TiO_2

Emmanuel Ngaha[a,*], Stéphanie Sayen[b], Emmanuel Guillon[b], Dilek Duranoğlu[a,*]

[a]*Chemical Engineering Department, Yildiz Technical University, Davutpasa Campus 34210, Esenler, Istanbul, Turkey, Tel. +90 212 383 4749; emails: emmangaha@gmail.com (E. Ngaha); dilekdur@gmail.com/dduran@yildiz.edu.tr (D. Duranoğlu)*
[b]*Institut de Chimie Moléculaire de Reims (ICMR), UMR CNRS 7312, Université de Reims Champagne-Ardenne, 51687 Reims Cedex 2, France, Tel. +33 326 91 85 15; emails: stephanie.sayen@univ-reims.fr (S. Sayen), emmanuel.guillon@univ-reims.fr (E. Guillon)*

Received 2 December 2018; Accepted 13 May 2019

ABSTRACT

Effective photocatalytic degradation of thiamethoxam (THX) at low concentration was achieved by using perlite supported TiO_2 composite material (PST). Box–Behnken experimental design method was employed in order to evaluate the effect of process parameters and also optimize them. Accordingly, effects of three process parameters (pH, load of PST [PT {g/L}], and air flow rate [AF {L/h}]) were investigated on two responses: (i) the THX degradation percentage after 270 min (DEG270 [%]) and (ii) the electric energy per order (EE/O [kWh/m^3]). THX degradation was improved by decreasing pH value and increasing air flow rate. Increasing load of PST increased the degradation percentage until a critical value of about 8 g/L, then caused a decrease. Statistically significant second-order polynomial models were developed by regression analysis of experimental data. Optimum conditions were obtained as follows: pH 4, PT 8.30 g/L and AF 18 L/h for an initial THX concentration of 1.46 ppm. These conditions led to a response of 87% ± 5% for DEG270 and 120 ± 21 kWh/m^3 for EE/O. Control experiments confirmed a good optimized process and reusability of PST without any regeneration step.

Keywords: Thiamethoxam; Photocatalytic degradation; Perlite; Process optimization; Box–Behnken design

1. Introduction

There is a concern about the presence of pesticides in natural water resources. These molecules can reach water (drinking, surface and groundwater) [1,2] through runoff from treated plants and soils [1,3]. Their presence in ecosystem is becoming a problem on a global scale since it could pose the threat to aquatic organisms in a term of mutagenicity and generate unknown effects to non-target organisms and humans [2,4]. Several water treatment methods are currently being investigated, including advanced oxidation processes (AOPs), which introduce hydroxyl radicals into the medium that unselectively attack organic molecules, mineralizing them into water and carbon dioxide [5,6]. AOPs have been shown to be particularly effective at detoxifying low concentrations of micro-organic pollutants such as pharmaceuticals and pesticides [7–9]. Heterogeneous photocatalysis with TiO_2 is an especially powerful AOPs [8] that has shown great potential as a low cost, environmental friendly and sustainable treatment technology providing "zero" waste in water/wastewater treatments. The main technical barrier, which impacts its commercialization is the recovery of catalyst TiO_2 nanoparticles after water treatment. Immobilization of TiO_2 nanoparticles onto the surface of particles could facilitate the filtration at the end of the

* Corresponding authors.

process. Numerous researchers have used support material to facilitate the separation after treatment without decreasing the photocatalytic efficiency of TiO_2. Activated carbon [10], natural clays [11], glass plates, steel fibers [12] glass slide [13] and perlite granules [12,14,15] have been used as support material. The high porosity of perlite granules allows them to stay afloat on the water surface, making them unique in the set of TiO_2 support materials for photocatalytic degradation [12].

Thiamethoxam (THX), a neonicotinoid insecticide, displays interesting properties: flexible application methods, favourable safety profile, low use rate, long-lasting residual activity and excellent efficacy for modern integrated pest management programs. However, THX is toxic, bioaccumulative and difficult to mineralize. It is a threat to surface and ground waters because of its polarity (log Kow = –0.13), high water solubility (4.1 g/L), low sorption in soils [16], and high leaching capability [2,9,17]. Very recently, Klarich et al. [2] reported for the first time the presence of THX and two other neonicotinoids in drinking water and demonstrated their persistence during conventional water treatment. In order to clean up water polluted with THX, it is, therefore, necessary to find effective methods. Photocatalytic degradation of THX has been effectively used in the literature. Žabar et al. [13] have proven that TiO_2 immobilized on glass slides was a good catalyst in terms of insecticide degradation. Mir et al. [4] demonstrated that THX photocatalysis followed a pseudo-first-order kinetics and could generate several intermediate products including clothianidin. Yang et al. [18] optimized the photocatalytic degradation kinetics of THX by using one-factor-at-a-time (OFAT) and central composite design based on the surface methodology. They evidenced those surface reactions with photon holes and OH on TiO_2 surface were responsible for THX photocatalytic degradation and also that the thiophene ring was the most active site reacting with reactive oxidative species.

There are few studies dealing with the study of photocatalytic degradation of THX, usually considering high THX initial concentrations: Žabar et al. [13] lead their study at 100 ppm, Mir et al. [4] used 26.3 ppm, and 5 ppm was investigated by Pena et al. [17] in the study of THX persistence in wastewater. To our knowledge, THX concentrations under 5 ppm were not examined in the existing studies, whereas it is known that the TiO_2 photocatalytic reaction rate is dependent on the contaminant concentration [11,18]. It is thus important to investigate the photocatalytic degradation process of THX at low concentrations (<5 ppm), especially as this pesticide was detected at a maximal concentration of about 0.2 ppm in drinking water [2].

Optimization of process conditions to achieve high photocatalytic degradation rate is another concern to be solved. Researchers have tried to solve it by using a classical approach such as initial factors and experimental approach [19]. There is now increasing recognition that traditional OFAT approach ought to be replaced by chemometric methods such as Box–Behnken experimental design (BBD) based on the statistical design of experiments (DOE) [19]. OFAT approach examines the effect of each parameter (catalyst dose, pH, temperature, air flow rate, etc.) individually; on the other hand, BBD also considers interaction effects between process variables by requiring fewer experiments.

To our knowledge, there is no previous study on THX degradation by using perlite supported TiO_2 and systematic optimization of THX photocatalytic degradation process. In this study, for the first time, perlite supported TiO_2 (PST) was used as photocatalyst for THX degradation at low concentration (1.46 ppm). Box–Behnken experimental design (BBD) technique was first employed in order to investigate the effects of selected process variables for photocatalytic degradation of THX. Three process parameters – pH, load of catalyst (PT) and air flow rate (AF)– were investigated in order to optimize the process conditions enabling maximum degradation percentage and minimum energy requirement.

2. Materials and methods

2.1. Materials

Titanium dioxide (Degussa P-25®) was supplied from Evonik Degussa Specialty Chemicals Co. Ltd., (Turkey). Expanded perlite, as photocatalyst support, was obtained from TAŞPER Perlit Company, Turkey. Thiamethoxam (purity > 99%) was purchased from Sigma-Aldrich (Germany) and was dissolved in distilled water in order to prepare a stock solution at 291.71 ppm (10^{-3} mol/L). For photocatalytic degradation experiments, 1.46 ppm THX solution (5×10^{-6} mol/L) was prepared by diluting the stock solution in distilled water. 0.20 μm nylon membranes from Sigma-Aldrich (Germany) were used for filtration since no THX was adsorbed during filtration.

2.2. Perlite supported TiO_2

PST was prepared in the same way as reported in our previous study [20]. First, expanded perlite was sieved to the particle size of 1–2 mm, then rinsed with distilled water with the aid of air bubbling (5 mL air/min) till no powder was detected in the filtrate, and dried in an oven at 105°C overnight. Then, PST was prepared as follows: 2.4 g TiO_2 (Degussa P-25®) were added to 50 mL of absolute ethanol. After adding 5 mL of diluted nitric acid (at pH 3.3), the suspension was placed in an ultrasonic bath for 15 min in order to provide homogeneity. Then, 6 g of expanded perlite (diameter 1–2 mm) were added to the mixture while stirring for 10 min at 130 rpm. Next, the mixture was kept in ultrasonic bath for 15 min to disperse the possible flocculated TiO_2 powder. After drying in an oven at 120°C for 12 h, the mixture was calcined at 450°C for 1 h to provide a stronger adherence between perlite and titanium dioxide powder. After being cooled in a desiccator, PST was washed in distilled water under air bubbling for few minutes in order to remove titanium dioxide powder which had not been precipitated on perlite surface. After filtration and drying in an oven at 120°C for 4 h, PST was ready to use in photocatalytic degradation experiments. Zeiss EVO LS 10 (Germany) scanning electron microscope (SEM) was used to characterize the surface morphology. The crystalline structures were investigated with using Cu Kα radiation. The surface area of perlite and PST sample was measured using a Quantachrome Quadrasorb SI surface analyzer

(Boynton Beach, Florida, USA). Specific surface area was calculated using Brunauer, Emmett, and Teller equation for N_2 adsorption data between 0 and 0.3 relative pressure ranges.

2.3. Adsorption and photocatalytic degradation experiments

Adsorption kinetic studies were carried out by using the photoreactor (Fig. 1) as a batch reactor in dark condition in order to determine adsorption capacities of catalyst and also in order to differentiate both effects; adsorption and photocatalytic degradation process. The photoreactor temperature was kept at 20°C using a cooling water circuit. The photoreactor was covered with aluminium foil to block transition of light. In order to compare THX removal by TiO_2, perlite and PST; TiO_2 (1.15 g), perlite (2.85 g) and PST (4.00 g) was added to 500 mL of 1.46 ppm THX solution at natural pH (6.5). The mass of materials was chosen according to our previous study [14], which indicates that 4.00 g of PST contains 2.85 and 1.15 g of perlite and pure TiO_2, respectively. The obtained suspension was stirred at 400 rpm at 20°C during 300 min. Aliquots of 1 mL of the suspension were periodically collected from the reactor, filtrated using a 0.20 μm nylon membrane in order to remove particles, and the filtered solution was further analyzed by monitoring the absorbance at 252 nm by UV spectrophotometry (Analytik Jena Specord 200 Plus, Germany).

THX photocatalytic degradation experiments were carried out with 500 mL of 1.46 ppm THX in the photoreactor. The radiation source was 2 × 6 W UV lamps (365 nm). Before UV irradiation, the suspensions were allowed to stay in the dark for 30 min (predetermined equilibrium time) under stirring to reach the THX adsorption equilibrium onto PST surface. In order to optimize the photocatalytic degradation process, a series of photocatalytic degradation experiments corresponded to the 15 runs given in BBD matrix were performed. The initial solution pH was adjusted by using HCl or NaOH solutions.

2.4. Design of experiment

DOE provides to find a suitable relationship between a response and independent variables [21,22]. BBD was employed for the experimental design and optimization. BBD is well suited for fitting a quadratic surface, and usually works well for process optimization. It allows having a good modelling of the studied phenomena using second-order mathematical models [21,22]. A general second-order model is defined as follows:

$$y = a_0 + \sum_{i=1}^{n} a_i x_i + \sum_{i=1}^{n} a_{ii} x_i^2 + \sum_{i=1}^{n}\sum_{j=1}^{n} a_{ij} x_i x_j \Big|_{i<j} \quad (1)$$

where y is the theoretical response function, x_i and x_j are the design variables (independent variables or parameters or factors), a_i and a_{ij} represent the regression coefficients corresponding to the main factor effects and interactions, respectively, and n is the number of parameters [23,24]. JMP® 13 was used as DOE software. Three factors, pH of THX solution (pH), load of PST (PT) and air flow rate (AF), were chosen. The selected factors and levels can be seen in Table 1. The experimental matrix of BBD can be seen in Table 2.

2.5. Degradation efficiency and electric energy per order as responses

Two responses were selected for this study: THX degradation percentage after 270 min (DEG270 [%]) and electric energy per order (EE/O [kWh/m^3]). EE/O is defined as the number of kWh of electrical energy required to reduce the concentration of a pollutant by 1 order of magnitude (90%) in 1 m^3 of contaminated water [25–27]. The EE/O (kWh/m^3) can be calculated from Eq. (2):

$$\frac{\mathrm{EE}}{\mathrm{O}}\left(\frac{\mathrm{kWh}}{\mathrm{m}^3}\right) = \frac{\left(P \times t \times 10^3\right)}{V \times 60 \log\left(\frac{C_0}{C}\right)} \quad (2)$$

where EE/O is the electric energy per order, P is the rated power of the UV lamp (kW), V is the volume of treated water (L), t is the irradiation time (min), C_0 and C are THX concentrations (mg/L) before and after treatment, respectively.

2.6. Analysis of THX by LC-MS-MS

Degradation products were investigated by liquid chromatography-tandem mass spectrometry (Agilent 6200 Series TOF/6500 Series Q-TOF LC/MS System, Santa Clara, USA). An electrospray interface (ESI) was used for the MS and MS-MS measurements in positive ionization mode, and full scan acquisition was performed between m/z 50 and 1,000. A mixture of ultra-pure water (90%) and methanol (10%) was used as mobile phase at a flow rate of 0.4 mL/min in isocratic conditions using an Agilent HPLC Column Poroshell 3 × 50 mm × 2.7 μm Ec-c18 model. The limit of

Table 1
Process variables and their levels for the study of THX degradation using BBD

	Range and levels		
Factors	Low (–1)	Middle (0)	High (+1)
X_1: pH	4	6.5	9
X_2: PT (g/L)	6	8	10
X_3: AF (L/h)	6	12	18

Table 2
Experimental matrix used for BBD

	Pattern				Pattern				Pattern		
Run	X_1	X_2	X_3	Run	X_1	X_2	X_3	Run	X_1	X_2	X_3
1	–	0	–	6	0	–	–	11	0	0	0
2	0	+	–	7	+	–	0	12	0	–	+
3	+	+	0	8	0	0	0	13	–	–	0
4	0	0	0	9	+	0	–	14	0	+	+
5	+	0	+	10	–	0	+	15	-	+	0

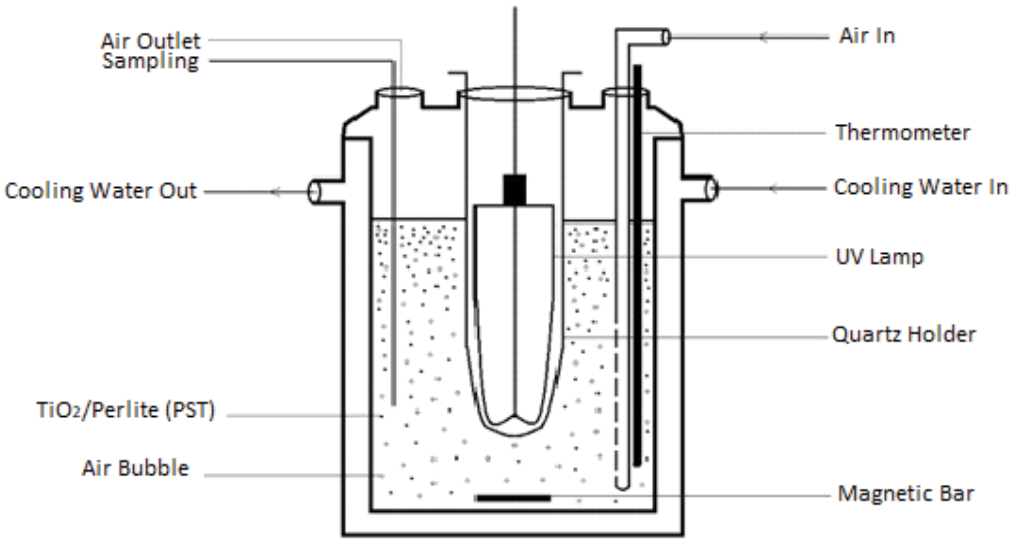

Fig. 1. Photoreactor

detection (LOD) (0.73 μg/L) was determined using the Sigma method by using Eq. (3), where σ is the standard deviation and *S* is the slope of the calibration curve. The limit of quantification (LOQ) was calculated with Eq. (4) as 2.19 μg/L.

$$\mathrm{LOD} = \frac{3.3\sigma}{S} \tag{3}$$

$$\mathrm{LOQ} = \frac{10\sigma}{S} \tag{4}$$

3. Results and discussion

3.1. Characterization of photocatalyst

The XRD pattern showed that anatase is the main crystalline phase for TiO_2 and PST samples (Fig. 2). No significant modification was observed after coating on perlite and calcination. Several researchers obtained the same results after coating and calcination for TiO_2/perlite [28] and for TiO_2/zeolite [29]. The specific surface area of perlite and PST was found as 9.11 and 18.32 m^2/g, respectively. The PST surface is almost twice larger than perlite due to the presence of TiO_2, of which surface area is 56 m^2/g [30].

In Fig. 3, are reported SEM images of TiO_2, perlite and PST, which evidenced a homogeneous coating of TiO_2 onto perlite.

3.2. Adsorption and photocatalytic degradation study

THX adsorption kinetics onto different solids (perlite, TiO_2 and PST) was studied in order to determine the corresponding adsorption equilibrium times. These preliminary experiments were also needed to distinguish between THX adsorption and photocatalytic degradation. Thus, experiments were performed for the three solids both in dark conditions (adsorption) and under UV light (photocatalytic degradation) after adsorption equilibrium time in dark conditions. Fig. 4 reported the relative concentration (C/C_0) of THX in the solution as a function of time. Concerning experiments in dark condition, it was determined that THX was not adsorbed on perlite, whereas after about 30 min (equilibrium time), about 10% and 18% of THX was adsorbed onto TiO_2 and PST, respectively.

The results after irradiation of THX solution (1.46 ppm, natural pH [6.5]) in the presence of PST and TiO_2 are also shown in Fig. 4. Concerning TiO_2, approximately 95% of THX degradation was achieved within 180 min of irradiation, and 90% of THX was degraded by using PST.

The degradation data fitted well with the Langmuir–Hinshelwood (L-H) model [8]. The simple term of the model is represented in Eq. (5), where *k* is the typical pseudo-first-order rate constant when the organic concentration is low (in mM), C_0 is the initial concentration and *C* is the concentration at time *t*. The *k* values were graphically determined and the THX half-lives ($t_{½}$) were calculated by using Eq. (6) (Table 3):

$$\ln\left(\frac{C_0}{C}\right) = kt \tag{5}$$

$$t_{\frac{1}{2}} = \frac{\ln 2}{k} \tag{6}$$

The pseudo-first-order rate constants, *k*, and the half-lives, $t_{½}$, for the different tested conditions given in Table 2 (runs 1–15) and for the experiment with pure TiO_2 (1.15 g at natural pH [6.5]) are reported in Table 3. As can be seen, $t_{½}$ values vary between 77 and 126 min (except TiO_2 data), and *k* values range from 41.21×10^{-4} to 90.00×10^{-4} min^{-1}. The fastest photodegradation kinetics (highest *k* and lowest $t_{½}$ values) was obtained with pure TiO_2 ($t_{½} \approx 39$ min) as expected, followed by PST at the conditions of run 6 (pH 6.5; PT 6 g/L

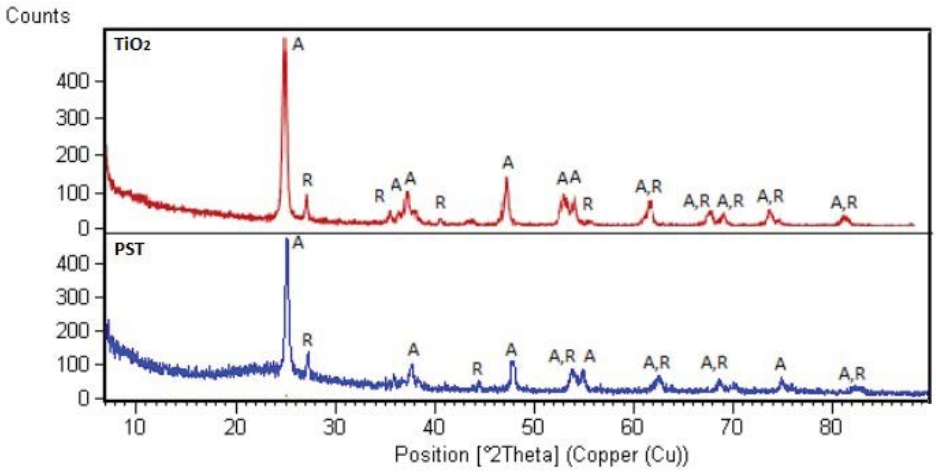

Fig. 2. XRD patterns of TiO_2 and PST.

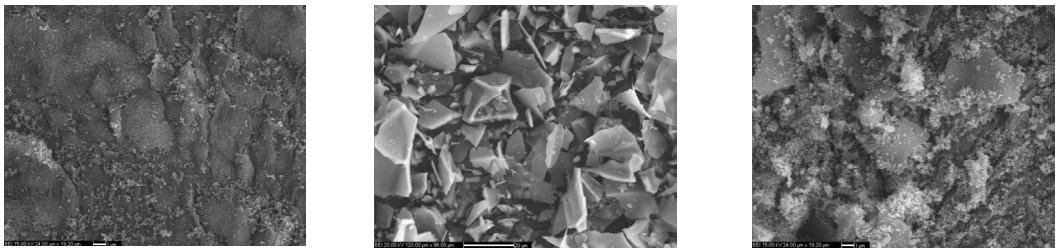

Fig. 3. SEM images of TiO_2 (5,000×), perlite (1,000×) and PST (5,000×) samples.

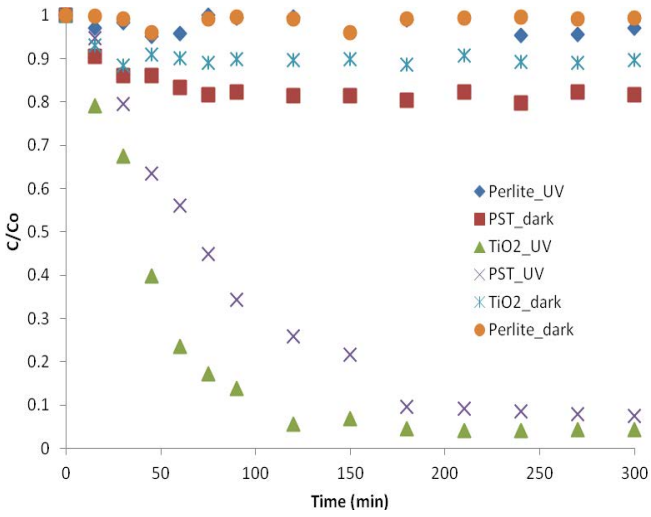

Fig. 4. Relative concentrations of THX in the presence of TiO_2, perlite or PST.

and AF 6 L/h) ($t_{½}$ ≈ 7 7 min). $t_{½}$ are 77.02 and 77.24 min for the runs 6 (0 – –) and 12 (0 – +), respectively. As can be seen, the only difference between these runs is air flow rate, which is 6 L/h for the run 6 and 18 L/h for the run 12. Therefore, it can be concluded that air flow rate has a weak effect on the half-lives.

3.3. Response surface modelling

BBD was used for the analysis of the photocatalytic degradation of THX. The DEG270 and EE/O values obtained after carrying out the experimental runs given in Table 2 are reported in Table 4. DEG270 values were found between 71.41% and 88.49%, EE/O values were between 115.01 and 198.63 kWh/m^3 at the studied conditions.

3.3.1. Development of regression model

The main objective of using BBD is to propose a regression model for the responses DEG270 and EE/O in this study. The quadratic models were used to find out the relationship between the responses and variables. The method of least squares was typically used to estimate the regression coefficients. *p*-value can be used to identify process parameters, which have a statistically significant effect on response. *p*-values less than 0.05 indicated that parameters are significant in 95% confidence interval (Table 5). It can be seen from Table 5 that the linear effects of pH, PT and some interaction effects (with the asterisk in Table 5) are significant.

The final empirical models for DEG270 and EE/O are given in Eqs. (7) and (8), respectively. The terms pH, PT and AF represent the coded values of the factors.

$$\mathrm{DEG270} = 84.26 - 2.83 \times \mathrm{pH} - 3.07 \times \mathrm{PT} + 1.43 \times \mathrm{AF} - 1.99 \times \mathrm{pH} \times \mathrm{PT} - 4.36 \times \mathrm{pH} \times \mathrm{AF} - 2.61 \times \mathrm{pH}^2 - 0.79 \times \mathrm{PT}^2 - 2.62 \times \mathrm{AF}^2 \quad (7)$$

Table 3
Rate constants (k), half-lives ($t_{½}$) and determination coefficients (R^2) for THX photocatalytic degradation

Run	1	2	3	4	5	6	7	8
k ($\times 10^{-4}$ min^{-1})	59.18	64.35	66.92	41.21	50.60	90.00	59.07	76.36
$t_{½}$ (min)	117.12	107.72	103.58	168.19	136.97	77.02	117.34	90.77
R^2	0.9862	0.9852	0.9906	0.9869	0.9850	0.9428	0.9796	0.9690
Run	9	10	11	12	13	14	15	TiO_2
k ($\times 10^{-4}$ min^{-1})	62.62	62.11	54.95	89.74	64.50	82.92	71.31	179.95
$t_{½}$ (min)	110.70	111.61	126.14	77.24	107.46	83.590	97.20	38.52
R^2	0.9933	0.9799	0.9702	0.9919	0.9766	0.9540	0.9897	0.9885

Table 4
BBD matrix of three variables in coded and actual values with experimental (Exp) and predicted (Pred) responses

Run	Coded values (X_1; X_2; X_3) (pH; PT; AF)	Actual values			DEG270 (%)			EE/O (kWh/m^3)		
		pH	PT (g/L)	AF (L/h)	Exp	Pred	Error (%)	Exp	Pred	Error (%)
1	− 0 −	4	8	6	75.95	75.62	0.33	174.52	175.92	1.39
2	0 + −	6.5	10	6	79.02	76.81	2.21	159.25	169.84	10.59
3	+ + 0	9	10	12	71.41	72.08	0.67	198.63	194.71	3.92
4	0 0 0	6.5	8	12	83.82	84.26	0.44	136.52	137.83	1.31
5	+ 0 +	9	8	18	73.39	73.72	0.33	187.82	186.43	1.39
6	0 − −	6.5	6	6	80.81	82.05	1.24	150.63	144.25	6.38
7	+ − 0	9	6	12	85.40	83.09	2.31	129.24	140.16	10.92
8	0 0 0	6.5	8	12	85.62	84.26	1.36	138.23	137.83	0.40
9	+ 0 −	9	8	6	78.27	79.58	1.31	162.92	157.32	5.60
10	− 0 +	4	8	18	88.49	87.18	1.31	115.01	120.61	5.60
11	0 0 0	6.5	8	12	83.35	84.26	0.91	138.73	137.83	0.90
12	0 − +	6.5	6	18	83.16	84.90	1.74	139.60	131.15	8.45
13	− − 0	4	6	12	82.73	82.06	0.67	141.59	145.51	3.92
14	0 + +	6.5	10	18	80.42	79.66	0.76	152.49	156.74	4.25
15	− + 0	4	10	12	80.30	82.61	2.31	153.05	142.14	10.92

Table 5
Estimated regression coefficients for DEG270 and EE/O

Parameter	DEG270 (%)			EE/O (kWh/m^3)		
	Estimate	Standard error	p-Value	Estimate	Standard error	p-Value
Constant	84.2633	1.416705	<0.0001*	137.8267	6.584766	<0.0001*
pH	–2.8263	0.867551	0.0173*	13.8863	4.032329	0.0137*
PT (g/L)	–3.0700	0.867551	0.0122*	14.87625	4.032329	0.0102*
AF (L/h)	1.4263	0.867551	0.1513	–6.5500	4.032329	0.1554
pH × PT	–1.9875	1.226903	0.1564	10.3200	5.702574	0.1203
pH × AF	–4.3550	1.226903	0.0121*	21.1025	5.702574	0.0101*
pH × pH	–2.6142	1.277001	0.0866	–11.6067	5.935427	0.0983
PT × PT	–0.7867	1.277001	0.5605	2.0317	5.935427	0.7438
AF × AF	–2.6242	1.277001	0.0857	10.6342	5.935427	0.1234

*Significancy is higher than 95%.

$$\frac{EE}{O} = 137.83 + 13.89 \times pH + 14.88 \times PT - 6.55 \times AF + 10.32 \times pH \times PT + 21.10 \times pH \times AF - 11.61 \times pH^2 + 2.03 \times PT^2 + 10.63 \times AF^2 \quad (8)$$

3.3.2. Analysis of variance

According to the analysis of variance (ANOVA) given in Table 6, regression models are significant, and obtained *F*-value (7.4029 for DEG270 and 8.1540 for EE/O) and *p*-value, inferior to 0.05, (0.0126 for DEG270 and 0.0098 for EE/O) indicate that the models are in agreement with the experimental results at 95% confidence level, that is, there is only a 1.26% and 0.98% chance of error in the model of DEG270 and EE/O, respectively (Table 6).

3.3.3. Model fitting and error estimation

Fitting of the model to the experimental data was examined with the error analysis. As can be seen from Table 4, error values are from 0.33% to 2.31% and from 0.40% to 10.92% for DEG270 and EE/O, respectively, that is, developed models fit well with the experimental data. In addition, fitted quality between experimental and predicted data obtained from JMP software, indicated that the models fit very well since all experimental points (except one) are within the 95% confidence zone (not shown as figure).

The correctness of the model was checked by the coefficient of determination (R^2). The values of R^2 is 0.91 and 0.92 for DEG270 and EE/O, respectively (Table 6). This indicates a relatively good predictability of the model for both DEG270 and EE/O. Therefore, it can be concluded that the two response surface models developed in this study (Eqs. (7) and (8)) are satisfactory for the prediction of DEG270 and EE/O, respectively.

3.3.4. Effect of process parameters

Effects of process parameters on THX degradation efficiency and electric energy per order was evaluated in terms of interaction plots, which were obtained from JMP® software (Figs. 5a and b). Interaction plots represent two factors simultaneously, by keeping other factors constant. Fig. 5 evidences that there is an interaction between pH and AF and also between pH and PT for both DEG270 and EE/O. At pH 6, DEG270 is high when AF is high, whereas degradation is low for the case of pH 9 even at a higher air flow rate. A similar trend was observed between pH and PT, while the interaction between PT and AF is negligible. pH has a distinctive effect on the other parameters due to the fact that

Table 6
ANOVA for THX photocatalytic degradation

Responses	Source	Degree of freedom	Sum of squares	Mean square	R^2	*F* ratio	Prob > *F*
DEG270	Model	8	276.95248	34.6191	0.91	7.4029	0.0126
	Error	6	28.05862	4.6764			
	Total	14	305.01109				
EE/O	Model	8	6312.5184	789.065	0.92	8.1540	0.0098
	Error	6	580.6228	96.770			
	Total	14	6893.1412				

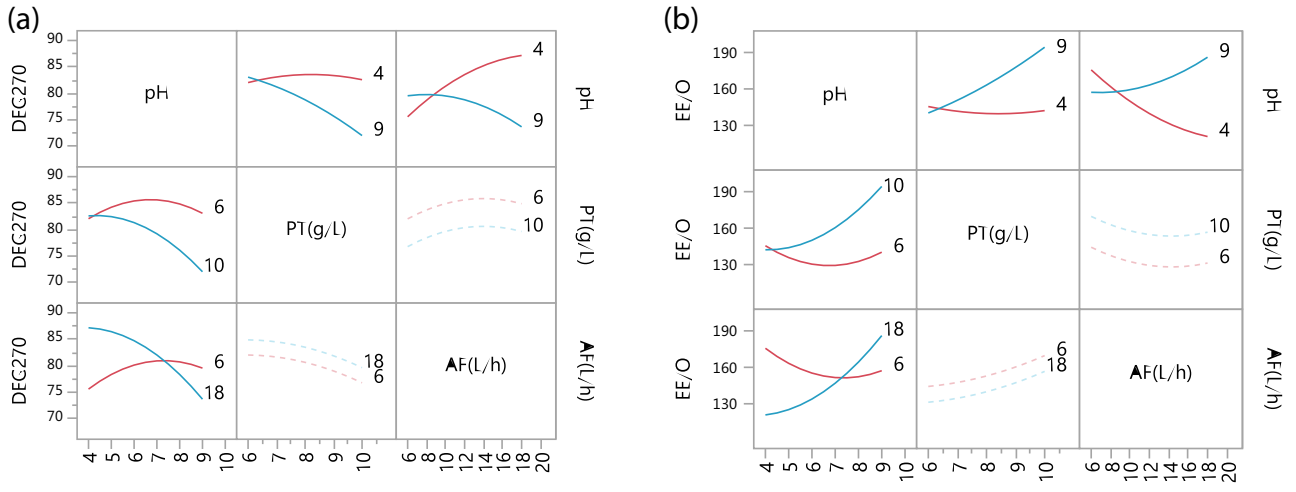

Fig. 5. Interaction plots between pH, PT and AF for DEG270 and EE/O.

the surface charge of the photocatalyst, size of aggregates and generation of oxidizing species are determined by pH [31]. Highest THX degradation efficiency and lowest electric energy consumption can be obtained at low pH and high AF conditions [31]. The rate of degradation increases with decrease in pH. This is compatible with the previous study performed on THX and other pesticides [31,32].

The effect of pH on photocatalytic oxidation performance can be explained by the point of zero charge (pH_{pzc}) [11,31]. At pH_{pzc}, the surface charge of TiO_2 is zero, and Degussa P25 used in this study has a pH_{pzc} at 6.9 [11,31]. At $pH < pH_{pzc}$, TiO_2 surface is positively charged and gradually exerted an electrostatic attraction force towards the negatively charged compounds. This intensifies the adsorption onto the photon activated TiO_2 surface for photocatalytic reactions [11,33]. The positive holes are considered as the main oxidizing species at low pH. In that case, the surface charge of TiO_2 is affected according to Eq. (9):

$$TiOH + H^+ \leftrightarrow TiOH_2^+ \quad (9)$$

At $pH > pH_{pzc}$ (TiO_2), the TiO_2 surface is negatively charged due to hydroxyl ions, thus, anionic compounds in water are repulsed. Eq. (10) shows the influence of the surface charge of the TiO_2 by pH:

$$TiOH + OH^- \leftrightarrow TiO^- + H_2O \quad (10)$$

Moreover, electron donor atoms such as nitrogen (5), oxygen (3), sulphur (1) and chloride (1) which are found in THX ($C_8H_{10}ClN_5O_3S$) may cause an increase of adsorption at $pH < pH_{pzc}$. It is also clear from Fig. 5 that an excess amount of PST in the system is adverse for the reaction, bringing out a negative influence on the photocatalytic efficiency and increased EE/O. This can be explained by blocking UV radiations by an excess amount of PST and their absorption by PST, and thus the low production of $OH^\bullet$ and $O_2^{\bullet}$ radicals, which are responsible for the degradation reaction. However, an excess amount of air provides higher efficiency, except at elevated pH. Air flow brings oxygen to the system and dissolved oxygen help to assure sufficient electron scavengers present to trap the excited conduction-band electron from recombination [11]. AF is also useful for mixing the solution for a better THX adsorption and UV absorption.

3.3.5. Response surface plots

3D response surface plots were used to evaluate the effects of selected variables on DEG270 and EE/O. The examination of surface plots as a function of two factors is the best way to check the relations between the factors and the response. It is clear that DEG270 is high at pH 4 and 18 L/h air flow rate (Figs. 6a and b) and EE/O is low at the same conditions (Figs. 6c and d). When increasing PT in a range of air flow between 10 and 18 L/h, the degradation percentage slightly increases before reaching a critical value and then decreases. In all cases, the degradation appears to be greater for PT values less than or equal to approximately 8 g/L (Fig. 6a). In acidic initial pH, the increase of the air flow causes an increase of DEG270 beyond 82% (Fig. 6b). With regard to EE/O, it can be seen from Fig. 6c that for PT values between 5.5 and 8 g/L, high air flow rates cause energy saving. The energy consumption is also minimal at high air flow rate and acidic conditions (Fig. 6d).

Since there were similarities between the information given by response surface plots, only the 3D surface plot of DEG270 and EE/O against PT and AF, and against pH and AF are shown in Figs. 6a–d, respectively.

3.3.6. Optimization

Response goals (maximization of DEG270 and minimization of EE/O) were used by JMP® to construct a desirability function. The desirability function indicates that the target goal is the most desirable. It can be said that the optimal conditions (reported in Table 7) are the best combination of factor settings for achieving the expecting responses. These results are conformed with those obtained from the surface plots (Fig. 6).

Photocatalytic degradation was set at optimum conditions and verified experimentally. As can be seen from Table 7, predicted values are closer to the experimental values. This confirms the suitability of the model for the prediction of process behaviour.

3.3.7 Stability and reusability of PST

Stability and reusability of PST were also studied by six photocatalytic degradation cycles. The photocatalyst was separated from the aqueous solution after each cycle, followed by washing with distilled water for two times and drying at room temperature for at least 12 h before the next usage. Then, the PST was used in the subsequent reaction under the same conditions. The activity of PST slightly decreased from 85% to 75% with the increasing repetition (Fig. 7). This fall can be explained by the loss of some fragments due to the weak mechanical strength of expanded perlite. However, PST could be used repetitively more than six times without significant deactivation and also without specific regeneration. To our knowledge, it was the first time that supported TiO_2 was used without any regeneration process. In addition, for the recovery of photocatalysts, PST can be collected from the aqueous media by simple flotation process easily.

3.4. Intermediate products research

LC-MS-MS and UV spectrophotometry analyses were conducted to identify the intermediate products generated during photocatalytic degradation. The total mineralization of THX can be mainly done via photocatalytic oxidation according to the stoichiometry proposed in Eq. (11).

$$C_8H_{10}ClN_5O_3S + \frac{33}{2}O_2 \rightarrow 8CO_2 + 5NO_3^- + SO_4^{2-} + Cl^- + H_2O + 8H^+ \quad (11)$$

LC-MS-MS chromatograms of THX samples obtained before and after degradation experiment at optimal conditions (after 180 and 270 min) are given in Fig. 8. It can be

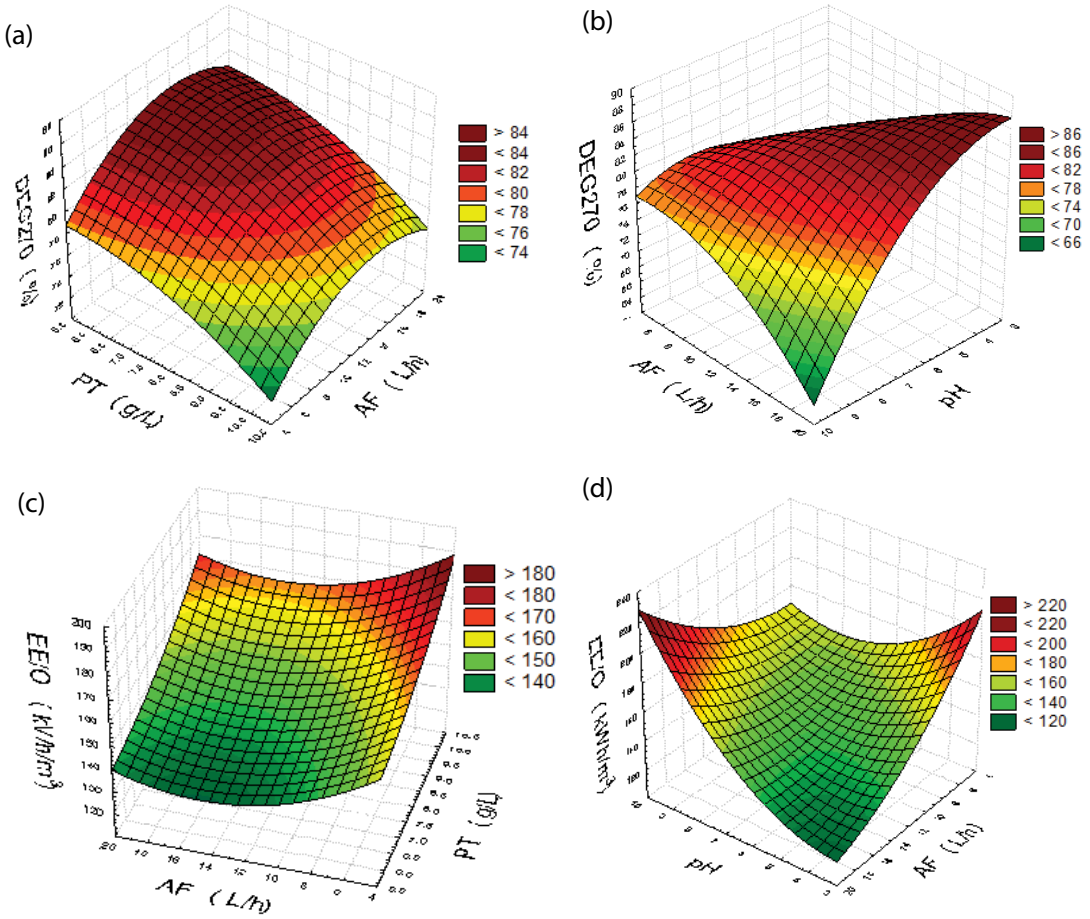

Fig. 6. 3D Surface plots (a) DEG270 against AF and PT, (b) DEG270 against pH and AF, (c) EE/O against AF and PT and (d) EE/O against pH and AF.

Table 7
Optimal conditions for THX photocatalytic degradation

Factors	Factor values	DEG270 (%)		EE/O (kWh/m^3)		Desirability
pH	4	Predicted	Experimental	Predicted	Experimental	
PT (g/L)	8.30	87	87 ± 5	120	120 ± 21	0.86
AF (L/h)	18					

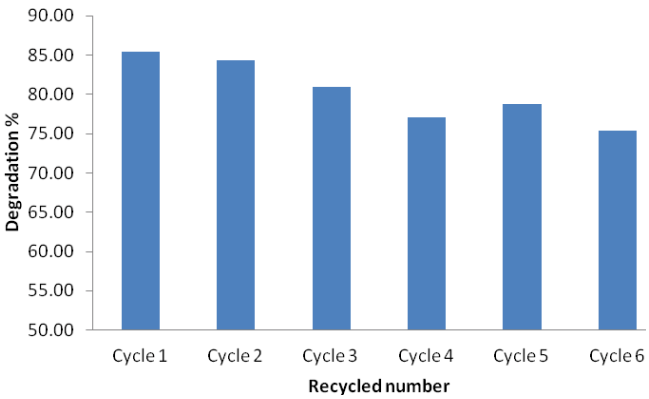

Fig. 7. THX degradation throughout the cycles.

seen from the figure that about 80% of the THX concentration decreased by 270 min of irradiation. Fig. 9 reports the corresponding mass spectra in the mass spectrum of the unirradiated THX sample, as it can be seen, there are no new peaks between m/z 100 and 350 after 180 and 270 min. The two main peaks, which appear in unirradiated sample, belong to THX combined with proton (m/z 292) and sodium (m/z 314). They are always present after 180 and 270 min of irradiation without other peaks but their intensity gradually decreased by about 80%, which is in good agreement with the degradation capacity (87%) given in Table 7. Although decomposition of THX was expected to release NO_3^- and SO_4^- as indicated in Eq. (12), these ions were not detected in the irradiated solutions of THX. This can be explained with incomplete mineralization of the pesticide and/or adsorption of degradation

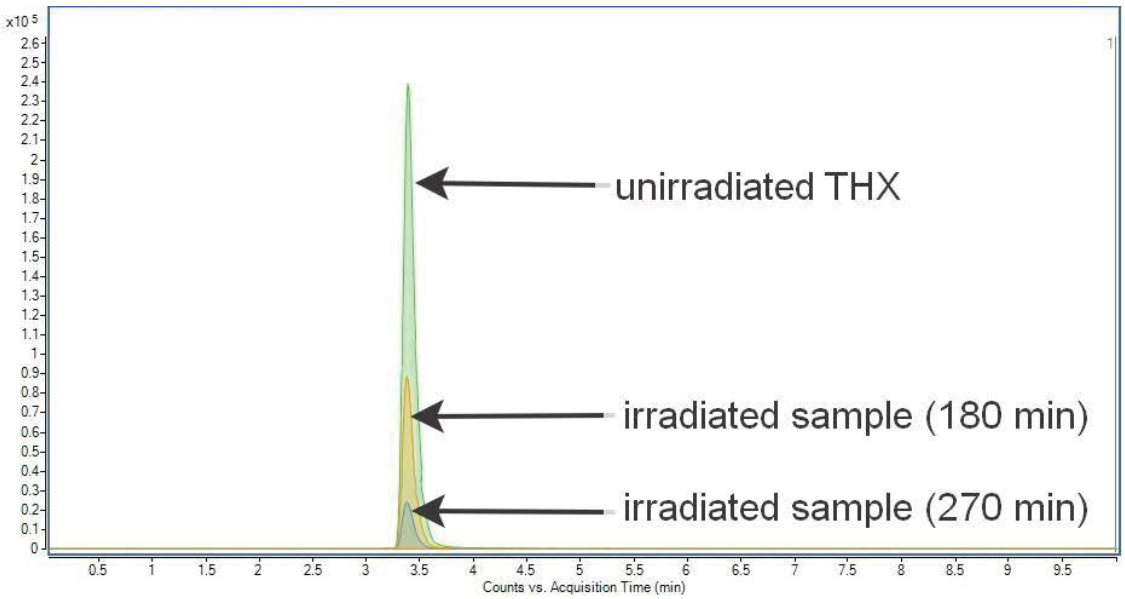

Fig. 8. Chromatograms of unirradiated THX and irradiated samples.

Table 8
Literature review of intermediate products of THX after photocatalytic degradation

$[THX]_0$ (ppm)	Method of detection	UV, wave length and power	Number of intermediate products	Photocatalyst	Irradiation period (min)	Reference
26.3	GC-MS	265 nm 125 W	12[a]	TiO_2 P25 (1 g/L)	360	[4]
100	LC-ESI-MS/MS	355 nm 6X20W	5[b]	TiO_2 60 mg/6 glass slides in 250 mL volume	120	[13]
1.46	LC-ESI-MS/MS	365 nm 2X6W	<LOD	TiO_2/perlite (8 g/L)	180 and 270	This work

[a]$C_8H_{10}ClN_5O_3S$, $C_7H_{12}ClN_5O_2S$, $C_9H_{12}ClN_3OS$, $C_8H_8ClN_5OS$, $C_5H_4ClN_3S$, $C_7H_9ClN_4OS$, $C_6H_9N_3O_3S$, $C_8H_{11}N_5O_2S$, $C_5H_{10}N_4O$, C_3H_3NO.
[b]$C_8H_{11}ClN_5O_3S$ (m/z: 292), $C_6H_8ClN_5O_2S$ (m/z: 250), $C_5H_4ClN_3O_2S$ (m/z: 292, 294), $C_6H_8ClN_3OS$ (m/z: 206, 208, 175, 205, 177), $C_8H_{10}ClN_3O_2S$ (m/z: 248, 250).

products onto the positively charged surface of PST, in acidic medium [34,35]. Partial mineralization is the most likely hypothesis according to the literature reported in Table 8, since, sulfur and nitrogen containing intermediate products are mentioned in all these studies. However, no intermediate product was detected in our working conditions (Fig. 9), which could be due to the low concentration (under LOD) of degradation products. Due to the different conditions such as applied wavelengths and UV sources (Table 8), it is not easy to compare these studies with ours. It is important to note that although 12 intermediate products have been determined by Mir et al. [4] with a short wavelength (265 nm) 125 W power lamp, long wavelength (355 nm) with similar power (120 W) lamp has led to totally different five intermediate products in Žabar et al. [13] study. In our study it was used 365 nm wavelength lamp with only 12 W power, then, any intermediate product was detected. The effect of wavelength and power on degradation products of THX photocatalytic degradation by PST can be investigated as future work.

4. Conclusions

The present study evidenced the potential of perlite supported TiO_2 as a photocatalyst for degradation of THX in aqueous solution. Box–Behnken experimental design was an efficient method for investigating the effect of process parameters on the photocatalytic degradation of THX. The quadratic model was developed and the statistical analysis showed a good fit for DEG270 (degradation percentage after 270 min) (with R^2 value of 0.91 and p-value of 0.0126) and for EE/O (required electric energy per order) (with R^2 value of 0.92 and p-value of 0.0098). We observed that the effect of initial pH and its interactions with PT (load of perlite supported TiO_2) and AF (air flow rate) are significant. PT has an optimum value of around 8.30 g/L. Effect of AF is also significant, increasing that parameter positively impact the process until 18 L/h. Thus, the optimal conditions were found as pH 4, PT 8.30 g/L and AF 18 L/h at the studied conditions. DEG270 was around 87% and, EE/O value was around 120 kWh/m^3

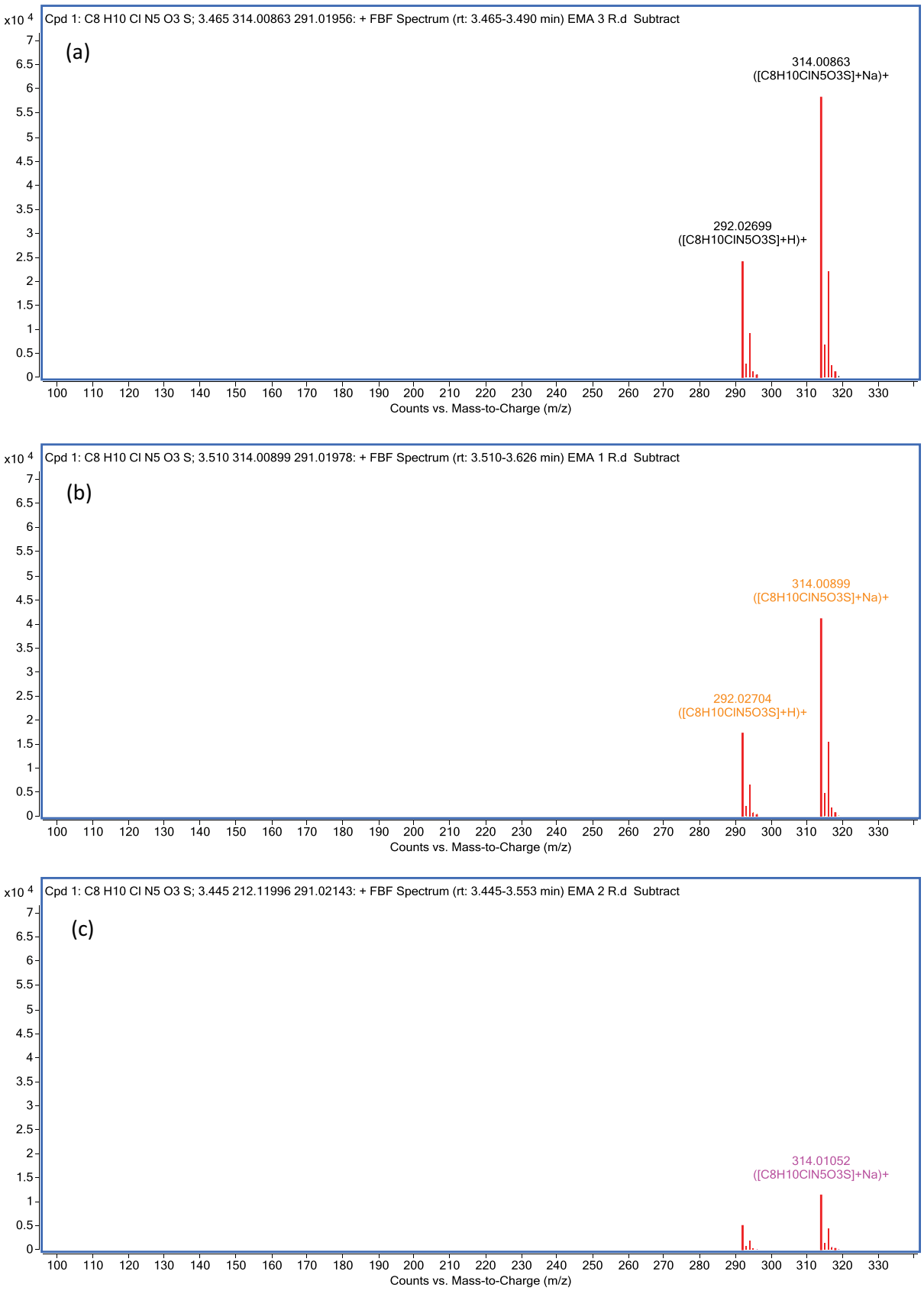

Fig. 9. Mass spectra of (a) unirradiated THX (1.46 ppm), and irradiated samples during, (b) 180 min and (c) 270 min at optimal conditions.

at the optimal conditions. The experimental results were in good agreement with those predicted by the model. The reusability of PST was also successfully tested without regeneration. After usage, separation of PST was easily achieved by flotation on the surface. As a conclusion, perlite supported TiO_2 presented suitable properties to be used as photocatalyst for degradation of thiamethoxam even at low concentration.

Acknowledgement

This study was supported by Yildiz Technical University Scientific Research Projects Coordinating Department (Project number: 2015-07-01-DOP02). The authors are also thankful to the Prime Ministry Presidency for Turks Abroad and Related Communities for their financial support.

References

[1] W. Aktar, D. Sengupta, A. Chowdhury, Impact of pesticides use in agriculture: their benefits and hazards, Interdiscip. Toxicol., 2 (2009) 1–12.
[2] K.L. Klarich, N.C. Pflug, E.M. Dewald, M.L. Hladik, D.W. Kolpin, D.M. Cwiertny, G.H. Lefevre, Occurrence of neonicotinoid insecticides in finished drinking water and fate during drinking water treatment, Environ. Sci. Technol. Lett., 4 (2017) 168–173.
[3] D. Landry, D. Dousset, F. Andreux, Laboratory leaching studies of oryzalin and diuron through three undisturbed vineyard soil columns, Chemosphere, 54 (2004) 735–742.
[4] N.A. Mir, A. Khan, M. Muneer, S. Vijayalakhsmi, Photocatalytic degradation of a widely used insecticide Thiamethoxam in aqueous suspension of TiO_2: adsorption, kinetics, product analysis and toxicity assessment, Sci. Total Environ., 458–460 (2013) 388–398.
[5] S. Malato, J. Blanco, J. Cácere, A.R. Fernández-Alba, A. Agüera, A. Rodríguez, Photocatalytic treatment of water-soluble pesticides by photo-fenton and TiO_2 using solar energy, Catal. Today, 76 (2002) 209–220.
[6] S. Mandal, Reaction rate constants of hydroxyl radicals with micropollutants and their significance in advanced oxidation processes, J. Adv. Oxid. Technol., 21 (2018) 178–195.
[7] H. Cao, X. Lin, H. Zhan, H. Zhang, J. Lin, Photocatalytic degradation kinetics and mechanism of phenobarbital in TiO_2 aqueous solution, Chemosphore, 90 (2013) 1514–1519.
[8] T. Leshuk, D. de Oliveira Livera, K.M. Peru, J.V. Headley, S. Vijayaraghavan, T. Wong, F. Gu, Photocatalytic degradation kinetics of naphthenic acids in oil sands process-affected water: multifactorial determination of significant factors, Chemosphore, 165 (2016) 10–17.
[9] Q. Zhao, Y. Ge, P. Zuo, D. Shi, S. Jia, Degradation of thiamethoxam in aqueous solution by ozonation: influencing factors, intermediates, degradation mechanism and toxicity assessment, Chemosphore, 146 (2016) 105–112.
[10] M.A. Vishnuganth, N. Remya, M. Kumar, N. Selvaraju, Photocatalytic degradation of carbofuran by TiO_2-coated activated carbon: model for kinetic, electrical energy per order and economic analysis, J. Environ. Manage., 181 (2016) 201–207.
[11] M.N. Chong, B. Jin, C.W.K. Chow, C. Saint, Recent developments in photocatalytic water treatment technology: a review, Water Res., 44 (2010) 2997–3027.
[12] S.N. Hosseini, S.M. Borghei, M. Vossoughi, N. Taghavinia, Immobilization of TiO_2 on perlite granules for photocatalytic degradation of phenol, Appl. Catal., B, 74 (2007) 53–62.
[13] R. Žabar, T. Komel, J. Fabjan, M.B. Kralj, P. Trebše, Photocatalytic degradation with immobilised TiO_2 of three selected neonicotinoid insecticides: imidacloprid, thiamethoxam and clothianidin, Chemosphore, 89 (2012) 293–301.
[14] D. Duranoğlu, Preparation of TiO_2/perlite composites by using 2^{3-1} fractional factorial design, J. Turkish Chem. Soc. Sect. A Chem., 3 (2016) 299–312.
[15] M. Giannouri, Th. Kalampaliki, N. Todorova, T. Giannakopoulou, N. Boukos, D. Petrakis, T. Vaimakis, C. Trapalis, One-step synthesis of TiO_2/perlite composites by flame spray pyrolysis and their photocatalytic behavior, Int. J. Photoenergy, 2013 (2013) 8 p.
[16] K. Banerjee, S.H. Patil, S. Dasgupta, D.G. Oulkar, P.G. Adsule, Sorption of thiamethoxam in three Indian soils, J. Environ. Sci. Health., Part B, 43 (2008) 151–156.
[17] A. Pena, J.A. Rodríguez-Liébana, M.D. Mingorance, Persistence of two neonicotinoid insecticides in wastewater, and in aqueous solutions of surfactants and dissolved organic matter, Chemosphore, 84 (2011) 464–470.
[18] H. Yang, H. Liu, Z. Hu, J. Liang, H. Pang, H. Yi, Consideration on degradation kinetics and mechanism of thiamethoxam by reactive oxidative species (ROSs) during photocatalytic process, Chem. Eng. J., 245 (2014) 24–33.
[19] V.A. Sakkas, Md.A. Islam, C. Stalikas, T.A. Albanis, Photocatalytic degradation using design of experiments: a review and example of the Congo red degradation, J. Hazard. Mater., 175 (2010) 33–44.
[20] D. Duranoğlu, E. Ngaha, An investigation on thermal and UV regeneration of TiO_2/perlite composites, J. Adv. Oxid. Technol., 21 (2018) 248–260.
[21] P.W.M. John, Statistical Design and Analysis of Experiments, SIAM Classics in Applied Mathematics, Philadelphia, 1971.
[22] S.C. Ferreira, R.E. Bruns, H.S. Ferreira, G.D. Matos, J.M. David, G.C. Brandao, E.G.P. da Silva, L.A. Portugal, P.S. dos Reis, A.S. Souza, W.N.L. dos Santos, Box-Behnken design: an alternative for the optimization of analytical methods, Anal. Chim. Acta, 597 (2007) 179–186.
[23] M. Hatami, M.C.M. Cuijpers, M.D. Boot, Experimental optimization of the vanes geometry for a variable geometry turbocharger (VGT) using a design of experiment (DoE) approach, Energy Convers. Manage., 106 (2015) 1057–1070.
[24] D. Montgomery, Design and Analysis of Experiments, 8th ed., John Wiley and Sons Inc., New York, 2013, pp. 15–20.
[25] M.A. Behnajady, B. Vahid, N. Modirshahla, M. Shokri, Evaluation of electrical energy per order (E_{EO}) with kinetic modeling on the removal of Malachite Green by US/UV/H_2O_2 process, Desalination, 249 (2009) 99–103.
[26] J.R. Bolton, K.G. Bircher, W. Tumas, C.A. Tolman, Figures-of-merit for the technical development and application of advanced oxidation processes, J. Adv. Oxd. Technol., 1 (1995) 13–17.
[27] J.R. Bolton, K.G. Bircher, W. Tumas, C.A. Tolman, Figures-of-merit for the technical development and application of advanced oxidation technologies for both electric- and solar-driven systems, Pure Appl. Chem., 73 (2001) 627–637.
[28] M. Hinojosa-Reyes, S. Arriaga, L.A. Diaz-Torres, V. Rodríguez-González, Gas-phase photocatalytic decomposition of ethylbenzene over perlite granules coated with indium doped TiO_2, Chem. Eng. J., 224 (2013) 106–113.
[29] S. Gomez, C.L. Marchena, M.S. Renzini, L. Pizzio, L. Pierella, In situ generated TiO_2 over zeolitic supports as reusable photocatalysts for the degradation of dichlorvos, Appl. Catal., B, 162 (2015) 167–173.
[30] K.J. Antony, R.B. Viswanathan, Effect of surface area, pore volume and particle size of P25 titania on the phase transformation of anatase to rutile, Indian J. Chem. Sect. A, 48 (2009) 1378–1382.
[31] J. Xiao, Y. Xie, H. Cao, Organic pollutants removal in wastewater by heterogeneous photocatalytic ozonation, Chemosphere, 121 (2015) 1–17.
[32] K. Sivagami, R.R. Krishna, T. Swaminathan, Optimization studies on degradation of monocrotophos in an immobilized bead photo reactor using design of experiment, Desal. Wat. Treat., 57 (2016) 28822–28830.
[33] Y. Xu, C.H. Langford, Variation of Langmuir adsorption constant determined for TiO_2-photocatalyzed degradation of acetophenone under different light intensity, J. Photochem. Photobiol., A, 133 (2000) 67–71.
[34] G.R.M. Echavia, F. Matzusawa, N. Negishi, Photocatalytic degradation of organophosphate and phosphonoglycine pesticides using TiO_2 immobilized on silica gel, Chemosphere, 76 (2009) 595–600.
[35] M. Abdullah, G.K.C. Low, R.W. Matthews, Effects of common inorganic anions on rates of photocatalytic oxidation of organic carbon over illuminated titanium dioxide, J. Phys. Chem., 94 (1990) 6820–6825.